

# Akkalkan Deposit of Bentonite Clays, Southeast Kazakhstan: Formation Conditions and Prospects for Technological Use

V. V. Nasedkin<sup>a, †</sup>, N. M. Boeva<sup>a, \*</sup>, and A. L. Vasil'ev<sup>b</sup>

<sup>a</sup>*Institute of Geology of Ore Deposits, Petrography, Mineralogy, and Geochemistry, Russian Academy of Sciences, Moscow, 119017 Russia*

<sup>b</sup>*National Research Center Kurchatov Institute, Moscow, 123182 Russia*

\*e-mail: boeva@igem.ru

Received September 21, 2017; revised October 11, 2018; accepted March 11, 2019

**Abstract**—The paper presents the results of studying bentonite clays of the Akkalklan deposit (Southeast Kazakhstan). Four main bentonite types are distinguished based on mapping: light gray mudstone, dark gray laminar and rubbly, waxy light brown and pale laminar, and black plastic clays. Their mineralogical study revealed a relationship between the crystal morphological features of the major rock-forming clay mineral and formation conditions and technological properties of bentonite material for use in various branches of industry.

**Keywords:** bentonite, montmorillonite, genesis, colloidal-sedimentary, simultaneous thermal analysis, transmission electron microscopy

**DOI:** 10.1134/S1075701519050064

## INTRODUCTION

Bentonite clays represent an strategically important material, which has been used successfully in agriculture, medicine, mining, construction, and other industries. The direction of their use depends on the crystal chemical features of the major rock-forming mineral: montmorillonite with the empirical formula  $(\text{Na,Ca})(\text{Al,Mg})_2\text{Si}_4\text{O}_{10}(\text{OH})_2 \cdot n\text{H}_2\text{O}$ . Its crystal structure is described by a monoclinic unit cell with spatial group  $C2/m$  ( $B2/m$ ) and broadly varying unit cell parameters depending on the chemical composition:  $a = 5.17 \text{ \AA}$ ,  $b = 8.94 \text{ \AA}$ ,  $c = 9.95 \text{ \AA}$ ,  $\beta = 99.54^\circ$  (Drits and Kossovskaya, 1990). The structure is made up of a three-layer sheet with two layers of  $\text{Si}_2\text{O}_5$  tetrahedra, which are linked by three apices and form a hexagonal network, and a sandwiched octahedral  $\text{Al}_2(\text{OH})_4$  layer linked by tetrahedral layers via their fourth apices (Fig. 1). These sheets are bonded by Van der Waals or electrostatic force. Variation in the ionic composition is an important feature of montmorillonite, e.g.,  $\text{Al}^{3+}$  and  $\text{Fe}^{3+}$  cations can substitute for  $\text{Si}^{4+}$  in tetrahedra, whereas  $\text{Mg}^{2+}$ ,  $\text{Fe}^{2+}$ ,  $\text{Fe}^{3+}$ ,  $\text{Li}^+$ ,  $\text{Ni}^{2+}$ , and  $\text{Cu}^{2+}$  can substitute for  $\text{Al}^{3+}$  in octahedra (Ferrage et al., 2005). Hydrophylicity or expansion ability is important for montmorillonite in industrial use. Hydroxyl groups penetrate intrasheet space, expand the unit cell parameter  $c$ , and increase the crystal size by several times. This feature of montmorillonite is

used for fracturing rock beds without explosives (Nasedkin, 2006).

All smectites display a correlation between the physical and chemical properties and their formation conditions. Typical features of certain genetic types have been identified from careful study of various deposits (Kirsanov, 1981). Bentonites in hydrothermal-metasomatic and volcanosedimentary deposits exhibit the best quality for industry (Christidis et al., 1995; Miz et al., 2017). They are also the most studied; however, recovery of bentonites from these deposits cannot mean global industrial demands.

The bentonite deposits in the east of the Kazakhstan fold zone were preliminarily attributed to the volcanosedimentary type (Kirsanov et al., 1981). Detailed study of the mineral composition and crystal morphological features of montmorillonite from bentonite clays of the Akkalkan deposit in Kazakhstan points to a continental terrigenous and colloidal-sedimentary deposit type. These bentonites formed in shallow lacustrine basins. In contrast to volcanosedimentary bentonites, sedimentary bentonites form as a result of redeposition and diagenetic alteration of the weathering products of eruptive, metamorphic, and sedimentary continental rocks and crystallization of their colloidal products. Owing to the diverse composition of the parental rocks, clays (their erosion products), as a rule, inherit this diversity (Kirsanov et al., 1981; Simik et al., 1997). Redeposited sedimentary

<sup>†</sup> Deceased.

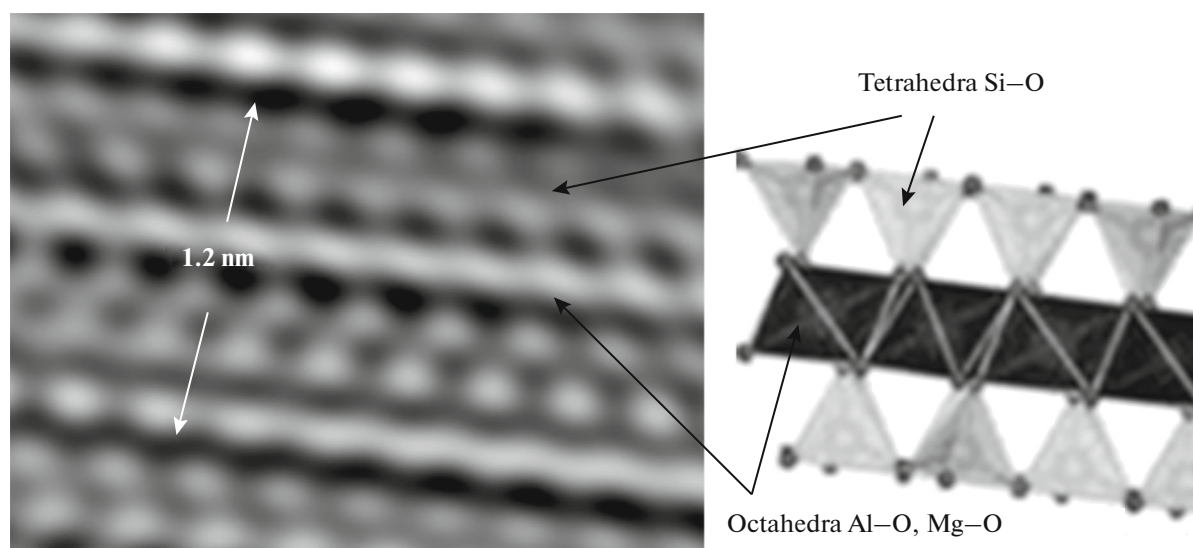


Fig. 1. Crystal lattice of montmorillonite: TEM image (left), schematic diagram (right).

bentonite deposits have a complex origin. All of them are confined to humid and arid lithogenesis zones.

In this paper, we present the results from studying the mineral composition of bentonite clays of the Akkalkan deposit using X-ray fluorescence, thermal, electron microscopic, and IR spectroscopic analyses, which allowed us to interpret the formation conditions of the deposit and to improve the ideas on bentonite quality and prospects for its use.

#### GEOLOGY OF THE REGION

The Akkalkan bentonite clay deposit is located in the Zaisan district of East Kazakhstan oblast, 110 km southeast of the town of Zaisan, and is confined to the western wall of the Kenderlyk foredeep. This foreland basin is a local third-order structure of the intermontane Zaisan depression that occurred between Dzhungaria and Altai (two large mountainous areas of Central Asia) on the Caledonian basement. The northern and southern walls of the basin are cut by large faults, which divide it from the Saikan Ridge in the north and the spurs of the Saur Ridge in the south. The Devonian sequences (tuffaceous molasse 700–3000 m thick and coastal marine carbonate–tuffaceous sediments 1000–3000 m thick) formed first, followed by Carboniferous porphyry albitophyres with sedimentary beds up to 1000 m thick (Kalugin et al., 1991). During orogenesis (Permian–Triassic), most sediments were eroded and latitudinal grabenlike troughs formed with coal-bearing rocks in the basement. The area of the deposit consists of Carboniferous, Permian, and Triassic rocks, which form the limb of a large syncline structure with a longitudinal strike (Fig. 2).

*Carboniferous rocks* of the Middle–Upper Carboniferous Kenderlyk Formation consist of sandstones,

siltstones, mudstones, and basalts with interlayers of kerogen rocks (lower subformation) and conglomerates, sandstones, siltstones, and kerogen rocks in the upper strata (upper subformation). The thickness of these rocks is ~200 m (Tsirel'son, 2006).

*Permian rocks* include three formations. The rocks of the Lower Permian Karaungur Formation in the lower part consist of intercalated layers of conglomerates, sandstones, siltstones, oil shales, limestones, and siliceous siderite rocks ~799 m thick. The intermediate and upper strata host sandstones intercalated with siltstones and mudstones and rare coal beds and lenses. The thickness of rocks is 330 m.

Bentonites are confined to the Middle Permian Tarancha Formation, the rocks of which include sandstones, siltstones, mudstones, and oil shale with lenticular horizons of dolomites, limestones, and siliceous siderite rocks.

The rocks of the Middle Permian Akkalkan Formation consist of intercalated siltstones, mudstones, and sandstones up to 230 m thick.

The *Upper Triassic rocks* of the Toresor Formation include conglomerates with interlayers of sandstones and siltstones ~900 m thick.

#### DESCRIPTION OF THE DEPOSIT AND BENTONITE CLAYS

The Akkalkan bentonite deposit was discovered in the 1970s. A horizon of bentonite clays 5–10 m thick is confined to the upper part of the Tarancha Formation and is traced as a continuous band to the south of the Akkolka River over a length of 3.5 km. Due to the steep dip, the bed cuts through all landforms, outcrops on top of hills, and vanishes in depressions beneath Quaternary sediments (Fig. 3). The dip angles of the

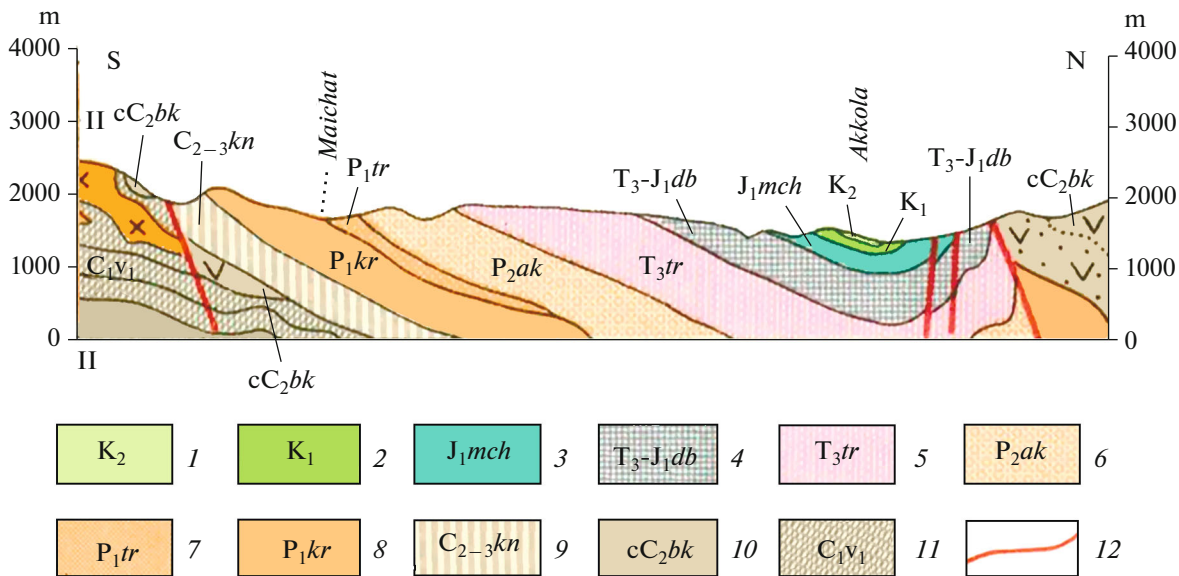


**Fig. 2.** Vertical cross section of Akkalkan bentonite deposit on scale of 1 : 200000. (1) Upper Cretaceous, brightly red gypsum-bearing clays, lenses of greenish sands, green clays, calcareous tuffs; (2) Lower Cretaceous, orange and brown conglomerates, sandstones; (3) Lower Jurassic, Mikhailovka Formation, siltstones, clayey and coal-bearing mudstones, sandstones, andesites, felsic tuffs; (4) Triassic–Jurassic, Dubovka coal-bearing Formation, siltstones, mudstones, coal-bearing mudstones, beds of brown coal, sandstones, gravelstones; (5) Upper Triassic, Toresor Formation, conglomerates, sandstones, subordinate green and lilac mudstones, coal beds; (6) Upper Permian, Akkalkan Formation, clayey and coal-bearing mudstones, coals, siltstones, sandstones, basal conglomerates; (7, 8) Lower Permian: (7) Tarancha Formation, fine-layered mudstones, oil shales; (8) Karaungur Formation, sandstones, mudstones, oil shales, tuffs; (9) Middle–Upper Carboniferous, Kenderlyk Formation, mudstones, lava, tuffs, basal conglomerates, oil shales, sandstones, tuffites, interlayers of dolomites and coal beds; (10) Middle Carboniferous, Bukon Formation, agglomerate and coarse-grained tuffs of porphyry andesites, andesites, basaltic andesites, tuffite sandstones, conglomerates, subordinate albitophyes; (11) Lower Carboniferous, Viscean Stage, lower substage, greywacke sandstones, siltstones, mudstones, clayey shales; (12) line of long-living tectonic contact and main faults (according to data of <http://webmapget.vsegei.ru>).

bentonite clay horizon vary from 40° in the north to 60°–70° in the south.

About ten latitudinal faults are distinguished at the deposit. In the present-day relief, they are expressed as dry creeks. Judging from the alluvial sediments, these creeks fill with water during strong rains and snowmelt. The boundaries between areas are typically expressed as steep cliffs. An evidently disrupted primary occurrence of rocks is locally observed along the transverse faults. The high-quality alkaline bentonite is confined to these zones.

A main bentonite clay bed 2 to 6–20 m thick is confined to the axial part of the ridge. Its external contacts are marked by bitumen and micaceous shales. The section is crowned by rubbly mudstones with numerous thin (2–3 to 10 cm) interlayers of oil shales. The bentonite bed is consistent and is divided into seven areas by transverse parallel faults.

*Area 1* (the northern part of the studied territory) is a conical highland with steep (30°–50°) slopes. The difference in elevation between the top and the base of the highland is 20–25 m. From west to east, the section includes dark gray rubbly–laminar mudstone ~10–15 m thick, rubbly mudstone with numerous inclusions of siliceous nodules (>15 m thick), light

gray mudstone of the productive layer (5–7 m thick), and coal-bearing rubbly mudstone with numerous thin interlayers of oil shales (>30 m thick) (Fig. 4). The light gray mudstone is crosscut by transverse fractures with acicular gypsum crystals.

*Area 2* hosts a bed of light brown waxy laminar bentonite (0.4–1.0 m thick) in the basement of outcropping strata, which is overlain by gray mudstone 3–4 m thick and identical to that located in the upper part of area 1. Gray mudstone is crowned by a thick (3–6 m) sequence of gray rubbly mudstone with siliceous nodules overlain by gray bentonite clays 5–7 m thick. These rocks form the main productive bed in the axial part of the ridge. The section is capped, as well as in the previous case, by rubbly mudstones with numerous thin (2–3 to 10 cm) interlayers of oil shales. In the south, the block terminates in a steep cliff. The length of the bentonite bed in this area is 170–180 m (Fig. 4). An outcrop exposed by mining exhibits rare transverse fractures with acicular gypsum crystals.

*Area 3*, with a length up to 40 m along strike, consists of two small domes of gray mudstone organic-matter-bearing clays similar to the main variety of the productive layer.



Fig. 3. Photo of outcrop of bentonite clay bed.

*Area 4* has a productive area 100 m long, 8–10 m thick, with two types of clays primarily distinct in color: dominant homogeneous light gray mudstone bentonites and subordinate cream, locally, brown clays, which form individual small bodies 1–2 to 3–4 m in size. Judging from the chemical composition, the brown color of bentonites is caused by a higher  $\text{Fe}^{3+}$  content. The spatial distribution of brown clays is relatively chaotic and probably depends on rock fracturing.

*Area 5* has a bentonite bed 120 m long and 2.0–2.5 m thick. The central part of the productive layer hosts numerous carbonate interlayers locally 1–2 cm thick.

*Area 6* is ~530 m long. In the northern part, for over a distance of 200 m, bentonite is whitish light gray and relatively hard. Farther south are rocks with typical waxy luster and specific laminar jointing, which are replaced by gray waxy bentonite with laminar jointing. The southern part of the area is a host to light gray mudstone clays with typical fine-laminar jointing, which are confined to a NW-trending fault. The thickness of this zone is ~10 m, and its length is 50–60 m. The central part of the area hosts black, plastic, strongly hydrated clays with a total area of  $15 \times 7$  m. The presence of water is probably related to leaking mineralized waters from an underground spring.

*Area 7* is located in the southern part of the deposit. The light gray bentonite bed is ~7 m thick and extends for over 50 m.

#### ANALYTICAL METHODS

The mineral composition of clays was studied by X-ray fluorescence and thermal analyses, transmission electron microscopy (TEM), and IR spectroscopy. For TEM, the clay samples were crushed in a mortar and mounted on standard electron microscopic grids with a carbon microhole film. The samples were studied on a Titan-80-300 (FEI, United States) transmitted/raster microscope (TEM/TREM) with a sample corrector at an accelerating voltage of 300 kV and light and dark field modes. The microscope is equipped with an EDAX system (United States) with a resolution of 128 eV.

Bentonite was also studied using simultaneous thermal analysis (STA). The differential scanning calorimetry (DSC) and thermogravimetry (TG) curves were simultaneously recorded on a NETZSCH STA 449 F3 Jupiter® analyzer. Prior to measurement, all samples were exposed in a desiccator for three days to achieve constant moisture. The analysis was conducted at a rate of  $10^\circ/\text{min}$  in atmospheric air in crucibles with closed caps up to  $1050^\circ\text{C}$ . The mass of the sampling was ~40 mg.

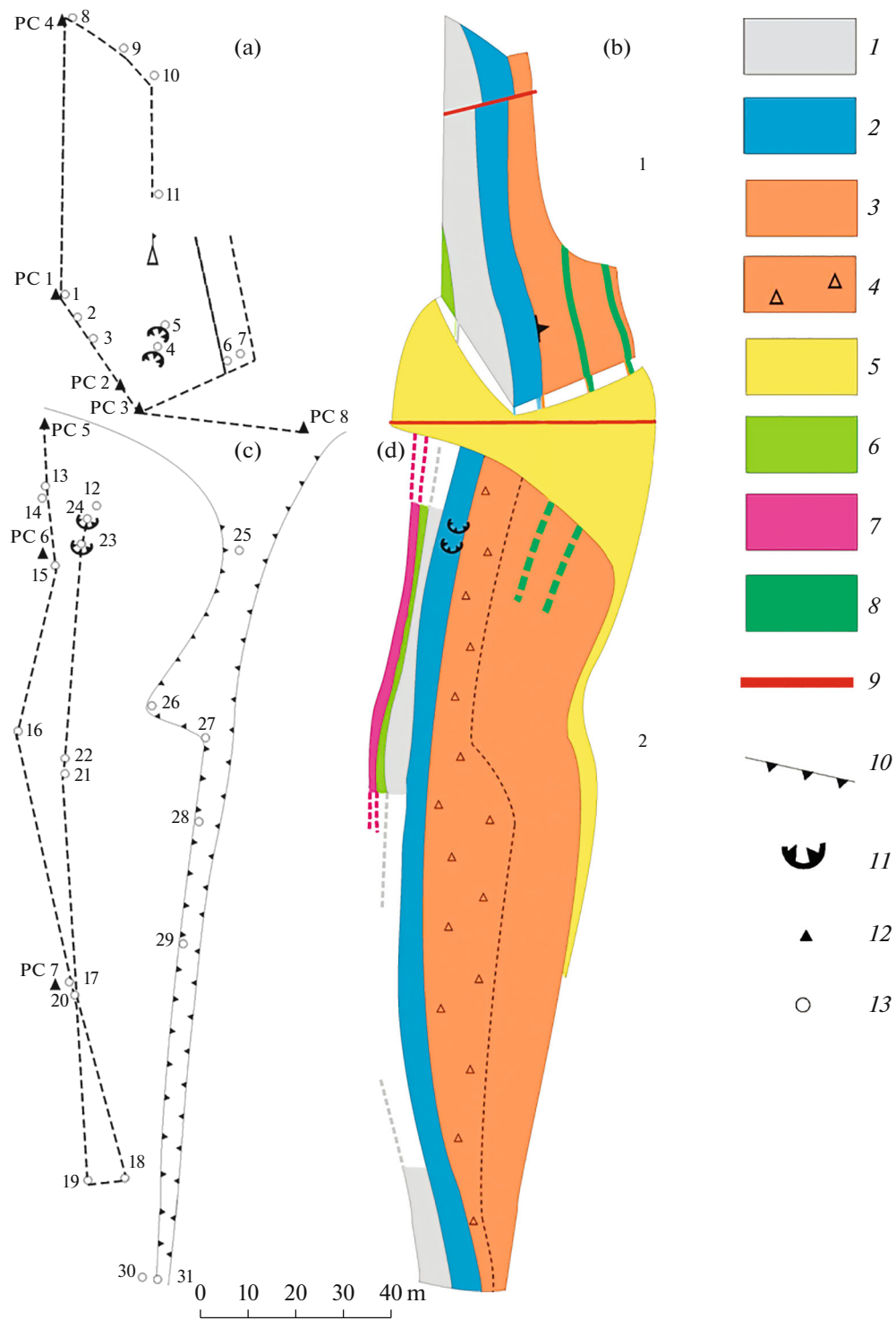


**Fig. 4.** Route (a, c) and schematic (b, d) geological map of areas 1 (a, b) and 2 (c, d) of Akkalkan deposit: (1) mudstones with siliceous boulders; (2) bentonite of central zone; (3) coal-bearing rubbly mudstone and shale; (4) eluvial-deluvial sediments of coal-bearing rubbly shale; (5) alluvial sediments; (6) rubbly-laminar bentonite; (7) laminar bentonite; (8) brown coal-bearing shale; (9) fault; (10) ravine; (11) extraction mines; (12) survey markers; (13) observation points.

The IR spectra were recorded on a Fourier high-sensitive spectrometer at the laboratory of microanalysis of the Institute of Organoelement Compounds, Russian Academy of Sciences (Moscow). Samples

were prepared as (i) bentonite tablets pressed in KBr and (ii) bentonite suspensions in Vaseline oil. The wavenumber range of 400–4000  $\text{cm}^{-1}$  is the most important for studying structural transformations of

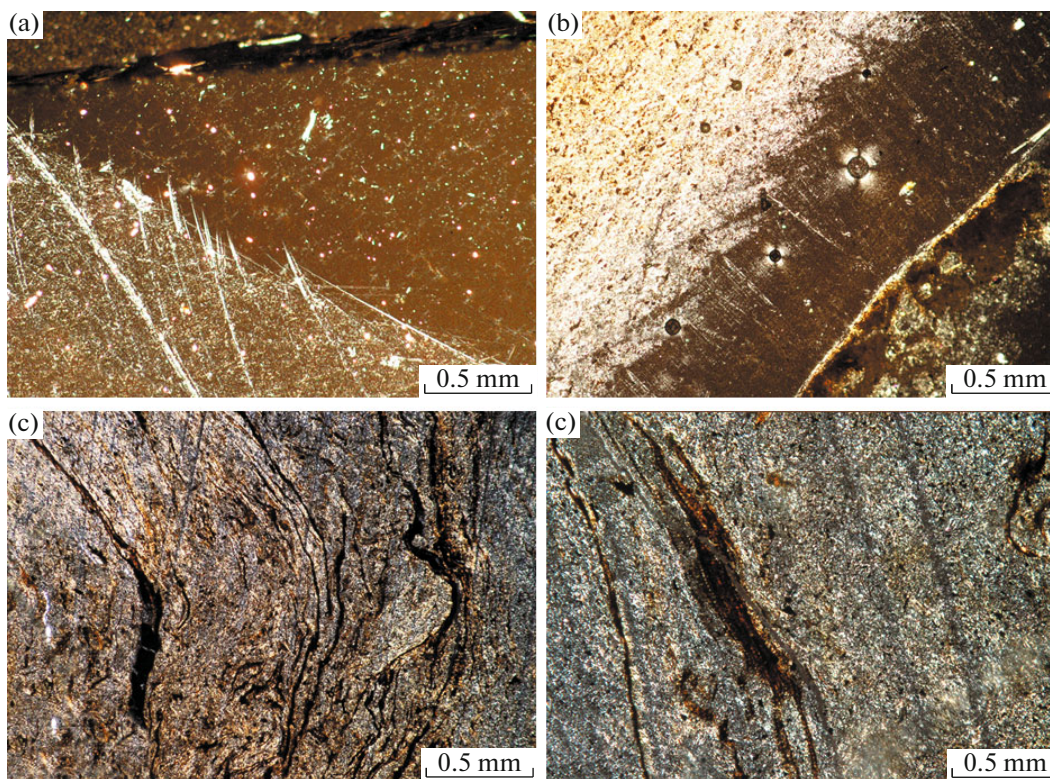


Fig. 5. Photomicrographs of smectite types of Akkalkan deposit: (a) Ak-1; (b) Ak-2; (c) Ak-3; (d) Ak-4.

montmorillonite upon heating. The wavenumber range of  $3000\text{--}3600\text{ cm}^{-1}$  makes it possible to study and identify OH groups, which are present in bentonite minerals at various stages of their transformations. The spectra were recorded for primary samples and samples heated at 300, 400, 500, and  $600^{\circ}\text{C}$ .

The chemical composition of clays was determined using an Axios RANalytical X-ray fluorescence spectrometer.

#### CHEMICAL AND MINERAL COMPOSITION OF BENTONITE CLAYS

Four main clay varieties were identified from petrographic, mineral, and chemical composition studies: light gray mudstone (Ak-1), dark gray with laminar and rubbly cleavage (Ak-2), waxy light brown and pale laminar (Ak-3), and black plastic (Ak-4) (Fig. 5).

##### *Light Gray Mudstone Clays (Ak-1)*

Banded light gray bentonites with acicular gypsum crystals are the main clay variety at this deposit (Fig. 5a). Approximately 50% of 60 samples of the deposit can be attributed to this type. The mineral composition of bentonite (vol %) includes montmorillonite (45–67), quartz (8–20), kaolinite (3–5), feldspar (5–6), and gypsum (0.5–1.5). The chemical composition of ben-

tonite is as follows (wt %): 67–70  $\text{SiO}_2$ , 0.1  $\text{TiO}_2$ , 12–14  $\text{Al}_2\text{O}_3$ , and 2–6  $\text{Fe}_2\text{O}_3$ . The cation exchange capacity (CEC) of montmorillonite is 84.21 mg-equiv/100 g.

The thermal curves exhibit four endothermic effects (Fig. 6a). The first effect is related to the extraction of absorption and interlayer water; at a maximum temperature of  $126.7^{\circ}\text{C}$ , montmorillonite loses 7.13% of its weight. This effect identifies the composition and character of hydrated exchange cations, because they affect the intensity and form of thermal effects. The complicated right shoulder of this effect indicates a mixed Na–Mg composition of exchange cations. The second endoeffect with greater intensity is related to dehydroxylation of kaolinite. The third endothermic effect of  $686.1^{\circ}\text{C}$  is responsible for the extraction of constituent water or hydroxyl in montmorillonite; it characterizes the thermal stability of the mineral due to partial amorphization. The second endoeffect has a second maximum at  $792^{\circ}\text{C}$  related to the position of certain octahedra or octahedral group relative to their dominant position. This is the basis for identifying trans- and cisoctahedra. The fourth endoeffect with a maximum of  $910.3^{\circ}\text{C}$  characterizes the complete decomposition of the layered silicate. The exoeffect with a maximum of  $965.8^{\circ}\text{C}$  confirms the presence of kaolinite in the sample (Boeva et al., 2013).

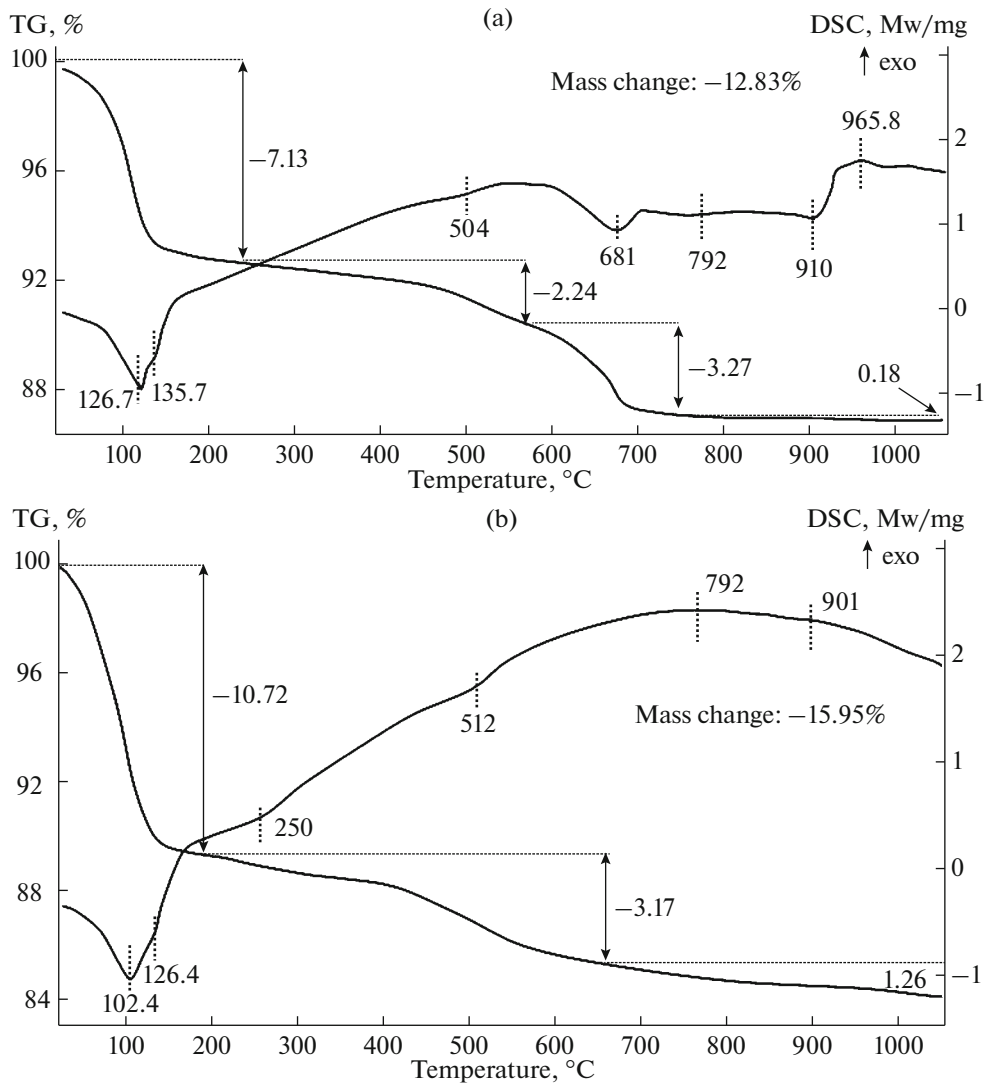


Fig. 6. Thermal curve of montmorillonite: (a) Ak-1; (b) Ak-2.

The influence of temperature on the behavior of water and hydroxyl in montmorillonite can be judged from the character of the IR spectra in the range of 3000–4000  $\text{cm}^{-1}$ . Bands at 3622–2627, 3400, and 3200  $\text{cm}^{-1}$  characterize hydroxyl of the octahedral layer, molecular water (valent O–H oscillations in water molecules from the hydrated cover), and poorly bonded water adjacent to the framework in montmorillonite particles, respectively. Sequential heating of sample up to 400°C causes a release of molecular water; the intensity of hydroxyl band remains unchanged. Intense extraction of hydroxyl from the octahedral layer is observed at 500°C. The IR spectroscopy data can trace the change in Me–OH groups of the montmorillonite octahedral layer. In the IR absorption spectra, this is reflected in the position of the band at 910  $\text{cm}^{-1}$ . After ignition of the sample at 550°C, this effect continues

to support the high thermal stability of Ak-2 bentonites (Boeva and Nasedkin, 2009).

In TEM, montmorillonite particles up to 1.0–1.5  $\mu\text{m}$  in size are scaly with rounded (Fig. 7a) and sharp fractured boundaries (Fig. 7b). Polycrystalline amorphous silica particles 1–2  $\mu\text{m}$  in size composed of grains 0.2–0.5  $\mu\text{m}$  in size are also found in samples.

#### *Dark Gray Laminar and Rubbly Clays (Ak-2)*

Microporous laminar bentonite consisting of montmorillonite and small clastic quartz grains (Fig. 5b), locally with organic matter occurs in the western part of the deposit. The pores are mostly made up of smectite. Bentonite consists of (vol %) montmorillonite (45–67), quartz (10–18), kaolinite (4–8), feldspar (3–6), hydromica (0–3), and gypsum (0.5–5.0). The chemical composition of bentonite is as follows (wt %):

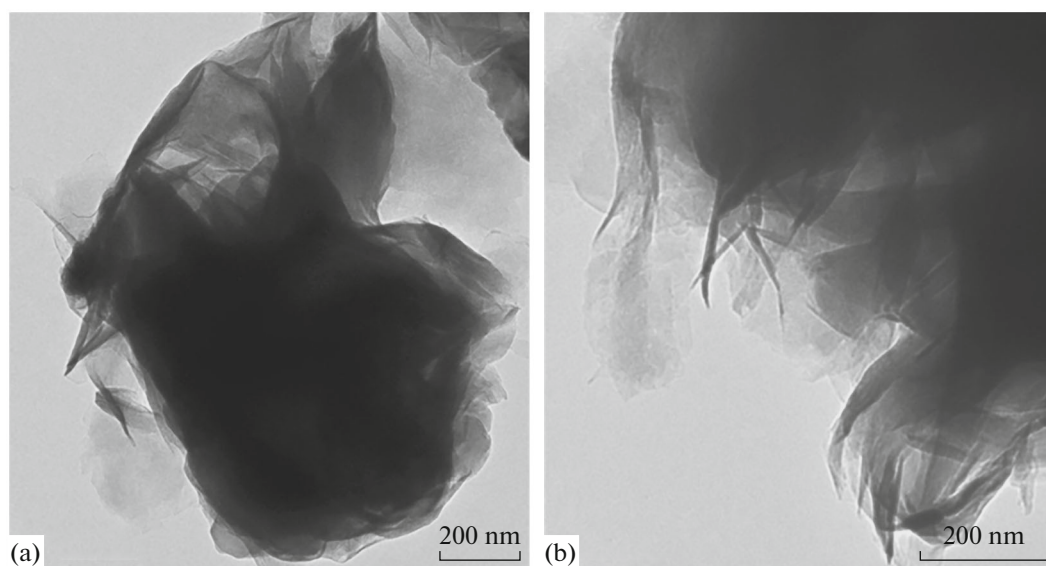


Fig. 7. Montmorillonite particles with smooth (a) and faulted (b) margins. TEM images.

59–62 SiO<sub>2</sub>, 0.3–0.5 TiO<sub>2</sub>, 13–20 Al<sub>2</sub>O<sub>3</sub>, and 2–5 Fe<sub>2</sub>O<sub>3</sub>. The CEC of montmorillonite is 101.75 mg-equiv/100 g.

The DSC curve exhibits three endoeffects (Fig. 6b). Montmorillonite is dehydrated in a range of 50–220°C losing 10.72% of its weight. Complication of the right shoulder of the endoeffect indicates the presence of two-valent cations Ca<sup>+2</sup> and Mg<sup>+2</sup> in the interlayer space of the mineral. The third endoeffect with a maximum at 512°C is related to dewatering of montmorillonite and kaolinite. It has a small intensity because it is overlapped by the flattened exoeffect with a maximum of 760°C responsible for dissociation of organic matter (Bortnikov et al., 2012). The temperature of this maximum indicates the high thermal stability of bentonite. A small endoeffect with a maximum of 1020°C corresponds to dehydroxylation of hydromica.

The IR spectra are characterized by bands at 3622–3637, 3400 and 3200 cm<sup>-1</sup> responsible for hydroxyl of the octahedral layer, molecular water, and poorly bonded water adjacent to the framework of montmorillonite particles, respectively. The IR data make it possible to trace the change in Me-OH groups of the octahedral layer, in particular, of montmorillonite. The IR absorption spectra show these changes reflected in the position of the band at 910 cm<sup>-1</sup>. Reflections at 1382 and 1385 cm<sup>-1</sup> are responsible for the presence of organic matter. These can be NO<sub>3</sub><sup>-2</sup> molecules of Na or ammonium saltpeter (Plyusnina, 1976).

In TEM, scaly montmorillonite particles ~0.2 μm in size (in plain view) and 10–15 nm thick are observed. The 1.2 nm thickness of some particles corresponds to the alkaline mineral type. High-resolution study of the mineral has revealed its perfect structure

without structural defects (Fig. 8). Some samples contain hydromica with an interlayer distance of 0.9 nm (Fig. 9).

#### *Waxy Light Brown and Pale Laminar Clays (Ak-3)*

Bentonite with typical schistose structure and curved fractures filled by goethite and illite (Fig. 5c) occurs in the western part of the “mudstone ridge.” Bentonite consists of (vol %) montmorillonite (75–77), quartz (6–12), kaolinite (4–15), and feldspar (1–6). Its chemical composition is as follows (wt %): 58–60 SiO<sub>2</sub>, 0.2–0.3 TiO<sub>2</sub>, 18–19 Al<sub>2</sub>O<sub>3</sub>, 2.0–2.6 Fe<sub>2</sub>O<sub>3</sub>, 2.14–2.30 Na<sub>2</sub>O, 1.98–2.3 MgO, 0.2–0.3 K<sub>2</sub>O, and 0.68–1.91 CaO. The higher Al<sub>2</sub>O<sub>3</sub> content is due to the higher amount of kaolinite group minerals. The CEC of montmorillonite is 66.42 mg-equiv/100 g.

The DSC curves of this bentonite type are similar to those of type Ak-1 and only differ in the composition of exchange cations of the montmorillonite interlayer space (Fig. 10a). The low-temperature endoeffect is clearly doubled, indicating dominant divalent cations in the montmorillonite interlayer space. The temperatures of the endoeffect maxima are 114 and 139°C. The temperature of maxima responsible for dehydroxylation of montmorillonite and complete breakdown of the mineral is 668 and 889°C, respectively.

#### *Black Plastic Clays (Ak-4)*

Black plastic clays with Na and Fe sulfates occupy an area 15 × 7 m in size in the southern part of the deposit and contain (vol %) montmorillonite (25–30), quartz (25–35), kaolinite (20–30), and feldspar (10–16). The chemical composition of bentonite is as



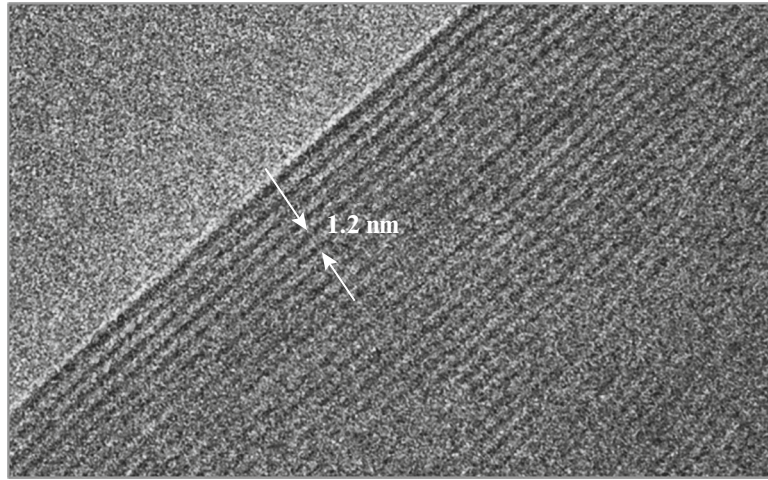


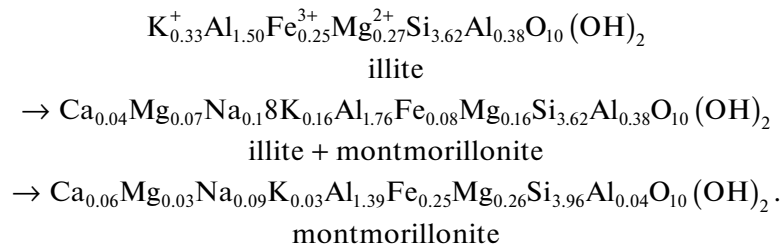
Fig. 8. Montmorillonite of sample Ak-2. High-resolution TEM image.

follows (wt %): 58–60 SiO<sub>2</sub>, 0.2–0.3 TiO<sub>2</sub>, 12–15 Al<sub>2</sub>O<sub>3</sub>, 2.0–2.6 Fe<sub>2</sub>O<sub>3</sub>, 1.14–1.8 Na<sub>2</sub>O, 1.98–2.30 MgO, 0.2–0.3 K<sub>2</sub>O, and 0.68–1.91 CaO.

The thermal curve of bentonite exhibits four endoeffects (Fig. 10b). The first has maximum of 105.9°C. Its form indicates the dominant Na cations in the interlayer montmorillonite space. Low enthalpy of dehydration of smectite (100 kJ/g) is related to compaction of layers of crystalline lattice as a result of argillic alteration. The second and third endoeffects with maxima of 504 and 651.3°C, respectively, are responsible for dehydroxylation of kaolinite and montmorillonite, respectively. The endoeffect in the range of 800–900°C characterizes the complete breakdown of the mineral. The flattened exoeffect starting at 300°C with a maximum of 792.5°C is responsible for combustion of organic matter. It overlaps the endoeffects of kaolinite and montmorillonite; thus, they are characterized by low intensity on the DSC curves. The exoeffect with a maximum of 985°C confirms the presence of kaolinite in the sample.

## DISCUSSION

The results of studying the mineral composition of bentonites and crystal morphological features of their major rock-forming mineral at the Akkalkan deposit evidence the relationship between the formation conditions and technological properties of bentonites. In the Permian, solonchak valleys with nonperennial salt lakes and sediments supplied by proluvial and alluvial flows formed under conditions of poorly dissected relief, high level of underground waters, and clay composition of rocks. The coarser sediments accumulated first, followed by fine-grained sediments. Mudstones formed during catagenesis as a result of reworking of sediments. Secondary crust formation occurred upon supergene alteration of rocks simultaneously with tectonic–denudation breaks. Sedimentary–hypogene processes, uplift of rocks of the Tarancha Formation on the Earth's surface in the post-Triassic, and interaction of mudstones with surface waters resulted in the formation of the major rock-forming mineral following the scheme: illite → illite + montmorillonite → montmorillonite (Garrels, 1984):



Transformation of illite with the formation of montmorillonite occurs due to the combination of hydrochemical and biological factors and includes two related mechanisms. First, the particles are torn to individual blocks. Mechanical stresses caused by intrusion of water monolayers into the interlayer space

results in breakdown of crystals. Further, their less ordered domains and illite–smectite phases pass into smectite (Krinari, 2011).

Bentonites and bentonite-like clays of the Akkalkan deposit form an ore zone more than 1.5 km long. Light gray clays 5–7 m thick (Ak-1), which are

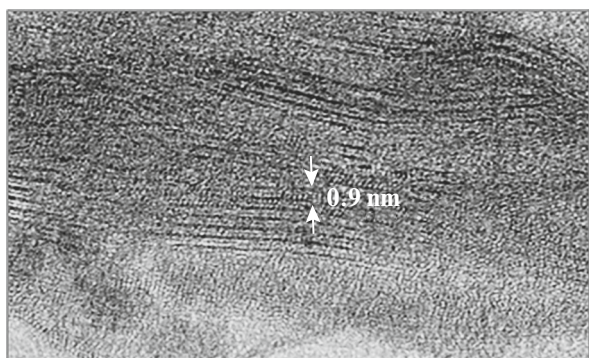


Fig. 9. Illite of sample Ak-2. High-resolution TEM image.

considered the main source of bentonites, crop out in the axial part of the ridge. There is distinct zoning related to primary coarse-grained sedimentation followed by fine-grained sedimentation. Zoning is expressed in the features of the mineral composition of bentonite and crystal morphological features of montmorillonite (from top to bottom): light gray mudstone clays (Ak-1), dark gray laminar and rubbly clays (Ak-2), waxy light brown and pale laminar clays (Ak-3), and black plastic clays (Ak-4). The contents of  $\text{SiO}_2$  and  $\text{Al}_2\text{O}_3$  increase and decrease, respectively, from top to bottom, due to the increasing amount of kaolinite in bentonite. The varying contents (wt %) of  $\text{Na}_2\text{O}$  (1.3–2.6),  $\text{MgO}$  (2.0–2.8),  $\text{K}_2\text{O}$  (0.4–0.8), and  $\text{CaO}$  (0.5–1.0) are related to the variable amount of K, Ca, Mg, and Na oxides. The higher  $\text{K}_2\text{O}$  content of some sam-

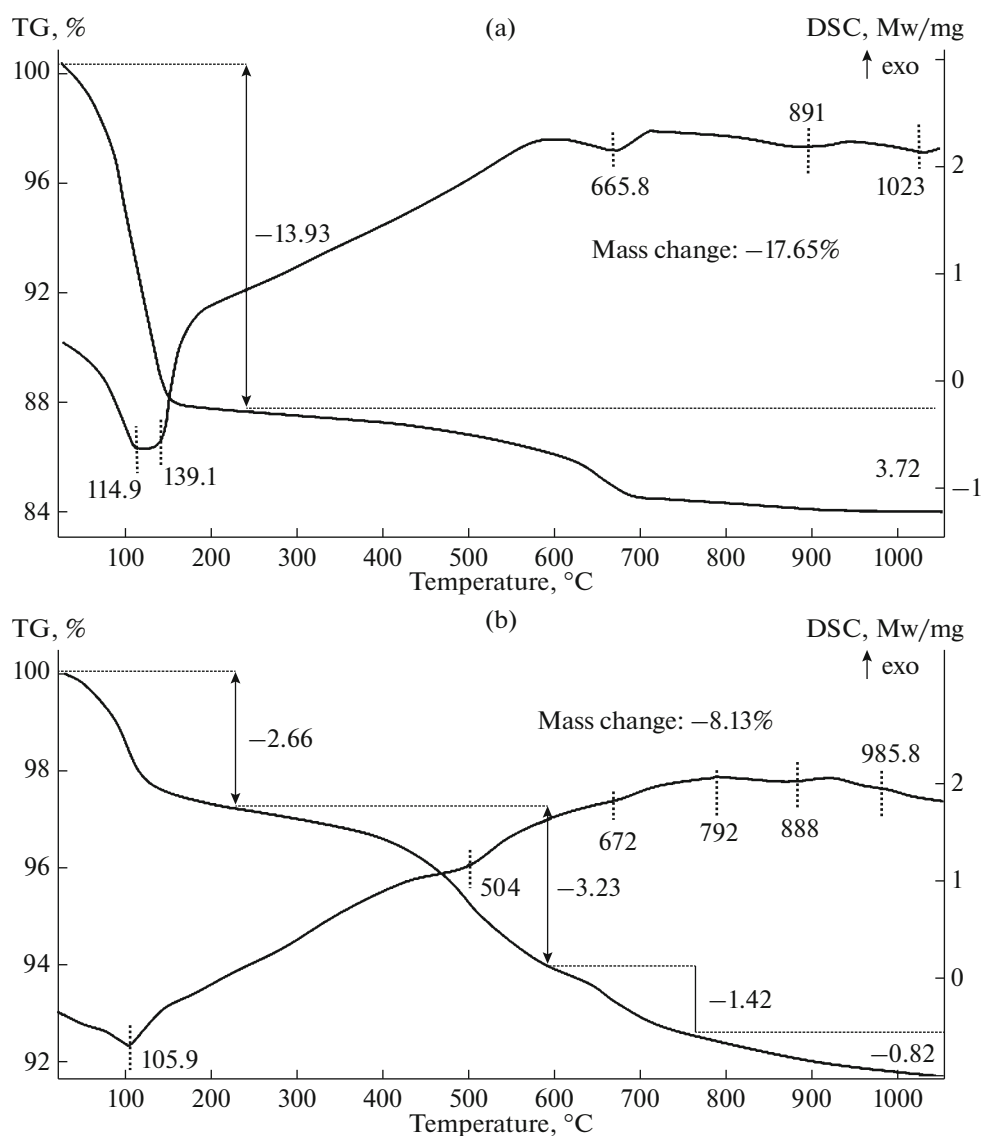


Fig. 10. Thermal curves of montmorillonite: (a) Ak-3; (b) Ak-4.

**Table 1.** Technological parameters of bentonite solutions (30 g/L)

Type	Soda, %	Polymer, %	Rheological characteristics by FANN viscosimeter									
			indications of viscosimeter						Apparent viscosity AV, mPa s	Plastic viscosity PV, mPa s PV	Flow point (Yield point) Yp, Pa	Density, $\rho$ , g/cm <sup>3</sup>
			$\varphi_{600}$ , rev/min	$\varphi_{300}$ , rev/min	$\varphi_{200}$ , rev/min	$\varphi_{100}$ , rev/min	$\varphi_6$ , rev/min	$\varphi_3$ , rev/min				
Ak-1	5	2	28	22	24.5	17.5	7	6	18	6	18	1.02
Ak-1	5	2	28	17	18	13	6.5	6	15	11	6	1.02
Ak-2	5.0	2	29	24	20.5	16	12	11	20.7	5	24	1.01
Ak-2	5	2	29	18	15	12	3	2	19.5	9	9	1.02
Ak-3	5	2	24	18	—	—	—	—	12.5	7	5.5	—
Ak-3	5	2	25	20	33	26	17	16	17.5	5	15.0	1.01
Ak-4	5	3	15	11	13	20.5	14.5	12.5	9	9	4	1.02
Ak-4	4.5	1	16	12	—	—	—	—	8	4	8	—

ples reflects a significant amount of hydromica. The Fe content is the lowest for the clayey rocks of the deposit (2.2–2.4%, no higher than 2.6%). Gypsum is identified only in the upper parts of the section in types Ak-1 and Ak-2. Amorphous silica particles have been found in clays Ak-1 during TEM studies. According to the CEC value of montmorillonite, the amount of divalent cations increases from top to bottom in the section. To the south, the thickness of clay beds decreases in fault-controlled areas.

Our studies have shown that the underlying rocks and the top rocks also contain thick clay varieties, which petrographically differ slightly from light gray mudstones but can expand and are rheologically similar to clays of the main productive layer. The thickness of expandable clays is significant, generally no less than 40 m.

#### PRACTICAL USE OF BENTONITE CLAYS

The bentonites of the Akkalkan deposit have been recommended for use in relatively small amounts as sorbents, mainly, in medicine. The use of Akkalkan bentonites in drilling, underground constructions, molding, and metallurgy stems from previous considerations.

As a result of our studies of the mineral composition of bentonite, we have assessed economic potential of the bentonite's quality. It was found that untreated mudstone clays are unusable in industry. Specific operations for determining the most favorable activation regime for bentonite were conducted based on the crystal chemical features of the rock-forming minerals of the clay types. The rheological properties of clay powders were analyzed before and after activation, the

parameters of which were selected experimentally (Table 1). The following scenario was adopted as optimal: 4.5–5% (of sample weight) of soda was added directly to a bentonite suspension. The viscosity parameters were measured on a Fann-35 device at  $\varphi_{600}$  and  $\varphi_{300}$ . The best results correspond to an activation soda solution temperature of 60–70°C. Then, as the crystals grow “older,” they slowly dissolve according to the cation exchange reaction  $\text{Ca}^{2+} + \text{Mg}^{2+} \rightarrow 2\text{Na}$ .

Ak-1 bentonites are suitable for drilling vertical boreholes. Ak-2 bentonites can be used for drilling horizontal and inclined boreholes. The composition of exchange cations and the content of the main rock-forming mineral indicate the high quality of this type (Table 1). Ak-3 bentonites meet the requirements of some subsurface operations, while Ak-4 bentonites are inapplicable for industrial use.

#### CONCLUSIONS

As a result of the comprehensive study of bentonites of the Akkalkan deposit, we identified the relationship between the clay mineral composition and crystal chemical features of montmorillonite and the formation conditions and technological properties of bentonite for use in various branches of industry. Alkali-earth bentonite formed in fresh lakes under reduced weakly alkaline or neutral conditions with a pH of 7–8. The lack of volcanic traces, the mineral composition of clays, and moderately ordered structure of montmorillonite indicate a colloidal-sedimentary type of deposit rather than volcanosedimentary. Zoning of bentonite types is related to redeposition and diagenetic alteration of the weathering products of the parental rocks. Because of their diverse composi-

tion, the clays (their erosion products), as a rule, inherit this diversity. Coarser-grained material was deposited first, and its transformation was less effective in contrast to finer-grained material typical of later sedimentation stages. The final stage included crystallization of colloidal products and the formation of montmorillonite.

The bentonites of the deposit are characterized by heterogeneous quality. The content of montmorillonite, illite, and quartz decreases with depth in contrast to the increasing amount of feldspar. Mapping has yielded four main types of bentonites, the quality of which becomes poorer from top to bottom: light gray mudstone, dark gray laminar and rubbly, waxy light brown and pale laminar, and black plastic clays.

#### FUNDING

The study was supported by State Contract no. 0136-2018-00525 of the Institute of Geology of Ore Deposits, Petrography, Mineralogy, and Geochemistry, Russian Academy of Sciences (IGEM RAS). Analytical studies were conducted at the IGEM ANALITIKA Center for Collective Use.

#### CONFLICT OF INTEREST

The authors declare that they have no conflict of interest.

#### REFERENCES

- Boeva, N.M., Bocharnikova, Yu.I., Nasedkin, V.V., and Belousov, P.E., Thermal analysis as express method of assessment of qualitative and quantitative characteristics of natural and synthesized organoclay, *Russ. Nanotekhnol.*, 2013, vol. 8, nos. 3–4, pp. 33–36.
- Boeva, N.M. and Nasedkin, V.V., Comparative characteristics of two genetic types of raw bentonite deposits, *Izv. Vyssh Uchebn. Zaved., Geol. Razvedka*, 2009, no. 6, pp. 27–31.
- Bortnikov, N.S., Novikov, V.M., Soboleva, S.V., Savko, A.D., Boeva, N.M., Zhegallo, E.A., and Bushueva, E.B., The role of organic matter in the formation of fireproof clay of the Latnenskoe Deposit, *Dokl. Earth Sci.*, 2012, vol. 444, no. 1, pp. 634–638.
- Christidis, G.E. and Huff, W.D., Geological aspects and genesis of bentonites, *Elements*, 1995, vol. 5, pp. 93–98.
- Drits, V.A. and Kossovskaya, A.G., *Glinistye mineraly: smektity, smeshanosloinye, obrazovaniya* (Clay Minerals: Smectites and Mixed-Layer Phases), Moscow: Nauka, 1990.
- Ferrage, E., Lanson, B., Sakharov, B.A., and Drits, V.A., Investigation of smectite hydration properties by modeling experimental X-ray diffraction patterns: Part 1. Montmorillonite hydration properties, *Am. Mineral.*, 2005, vol. 90, pp. 1358–1374.
- Garrels, R.M., Montmorillonite/illite stability diagrams, *Minerals*, 1984, vol. 32, no. 3, pp. 161–166.
- Kalugin, I.A., Tret'yakov, G.A., and Bobrov, V.A., *Zhelezorudnye bazal'ty v gorelykh porodakh Vostochnogo Kazakhstana* (Iron-Bearing Basalts in Burnt Rocks), Novosibirsk: Nauka, 1991.
- Kirsanov, N.V., Rateev, M.A., and Sabitov, A.A., *Geneticheskie tipy i zakonomernosti rasprostraneniya mestorozhdenii bentonitov v SSSR* (Genetic Types and Distribution of Bentonite Deposits in the USSR), Moscow: Nedra, 1981.
- Krinari, G.A. and Khranchenkov, M.G., Inverse transformation of secondary micas in sedimentary rocks: mechanisms and applications, *Dokl. Earth Sci.*, 2011, vol. 436, no. 2, pp. 262–268.
- Miz, M.T., Akichoh, H., Berraouan, D., Salhi, S., and Tahani, A., Chemical and physical characterization of Moroccan bentonite taken from Nador (north of Morocco), *Am. J. Chem.*, 2017, vol. 7, no. 4, pp. 105–112.
- Nasedkin, V.V., Bentonites as natural nanomaterial in building, *Stroitel'. Mater.*, 2006, no. 8, pp. 2–4.
- Plyusnina, I.I., *Infrakrasnye spektry mineralov* (Infra-Red Spectra of Minerals), Moscow: MGU, 1976.
- Simic, V., Djuric, S., and Zivotic, D., Bentonitic clays of the Drmno deposit (Kostolac coal basin), *Bull. Geol., Hydrogeol., Eng. Geol.*, 1997, no. 47, pp. 107–126.
- Tsirel'son, B.S., *Report on Results of Prospecting Works at the Akkalkan Project Area of Bentonite Clays for 2002–2005* (with Calculation of Reserves of Bentonite Clays at August 1, 2006).

*Translated by I. Melekestseva*